

ZNF238 Is Expressed in Postmitotic Brain Cells and Inhibits Brain Tumor Growth

Valérie M. Tatard¹, Chaomei Xiang¹, Jaclyn A. Biegel², and Nadia Dahmane¹

Abstract

Brain tumors such as medulloblastoma (MB) and glioblastoma multiforme (GBM) can derive from neural precursors. For instance, many MBs are thought to arise from the uncontrolled proliferation of cerebellar granule neuron precursors (GNP). GNPs normally proliferate in early postnatal stages in mice but then they become postmitotic and differentiate into granule neurons. The proliferation of neural precursors, GNPs, as well as at least subsets of GBM and MB depends on Hedgehog signaling. However, the gene functions that are lost or suppressed in brain tumors and that normally promote the proliferation arrest and differentiation of precursors remain unclear. Here we have identified a member of the BTB-POZ and zinc finger family, ZNF238, as a factor highly expressed in postmitotic GNPs and differentiated neurons. In contrast, proliferating GNPs as well as MB and GBM express low or no ZNF238. Functionally, inhibition of ZNF238 expression in mouse GNPs decreases the expression of the neuronal differentiation markers MAP2 and NeuN and downregulates the expression of the cell cycle arrest protein p27, a regulator of GNP differentiation. Conversely, reinstating ZNF238 expression in MB and GBM cells drastically decreases their proliferation and promotes cell death. It also downregulates cyclin D1 while increasing MAP2 and p27 protein levels. Importantly, ZNF238 antagonizes MB and GBM tumor growth *in vivo* in xenografts. We propose that the antiproliferative functions of ZNF238 in normal GNPs and possibly other neural precursors counteract brain tumor formation. ZNF238 is thus a novel brain tumor suppressor and its reactivation in tumors could open a novel anticancer strategy. *Cancer Res*; 70(3): 1236–46. ©2010 AACR.

Introduction

Brain development and tumorigenesis are highly related. The first involves the controlled proliferation and timely differentiation of precursors up to a certain stage, which is tightly controlled by developmental decisions, ensuring the formation of an appropriate brain, both in terms of size and shape. Tumorigenesis occurs as a result not only of the uncontrolled and/or uncoordinated action of proliferative and survival signals that bypass or override the normal mechanisms that restrict growth but also of the loss of restrictive signals that promote differentiation and block proliferation.

Medulloblastomas (MB) are cerebellar tumors that represent ~25% of all pediatric brain tumors (1, 2) and are thought to be derived largely from granule neuron precursors (GNP) in the cerebellar cortex. Glioblastomas multiforme (GBM), in contrast, arise mostly in adults and are often found

in the deep white matter. The survival rate of affected patients has been improved by current treatments such as surgery, radiotherapy, and chemotherapy; however, these can lead to severe neurologic deficits, especially in young children.

The mouse cerebellum is an excellent structure to investigate the relationship between normal development and tumorigenesis, and it shows a highly stereotyped and well-known architecture and development. In the first few weeks after birth, the cerebellar cortex is composed of four main layers defined as, from the outside to the inside, the external germinal layer (EGL), the molecular layer, the Purkinje layer, and the internal granular layer (IGL; see Fig. 1A; refs. 3–5). GNPs are derived from progenitors in the embryonic rhombic lip, which then migrate tangentially and cover the cerebellar anlage forming the EGL. During this process, GNPs proliferate rapidly, especially at early postnatal stages. After a defined number of divisions, they start to differentiate and migrate inward, crossing the molecular layer and the Purkinje layer to reach their final position in the IGL where they become mature neurons. When the correct numbers of GNPs and granule neurons are generated, the EGL decreases in size and is absent in adults.

A number of studies have highlighted the key role of the Sonic hedgehog (SHH) signaling pathway in the control of cerebellar growth (6–9). The SHH ligand is produced by Purkinje neurons and released into the EGL (3, 6–9), where it binds to the PATCHED1 (PTCH1) receptor on GNPs. This binding releases the inhibitory action of PTCH1 on the transmembrane

Authors' Affiliations: ¹The Wistar Institute; and ²Department of Pediatrics, The Children's Hospital of Philadelphia and University of Pennsylvania School of Medicine, Philadelphia, Pennsylvania

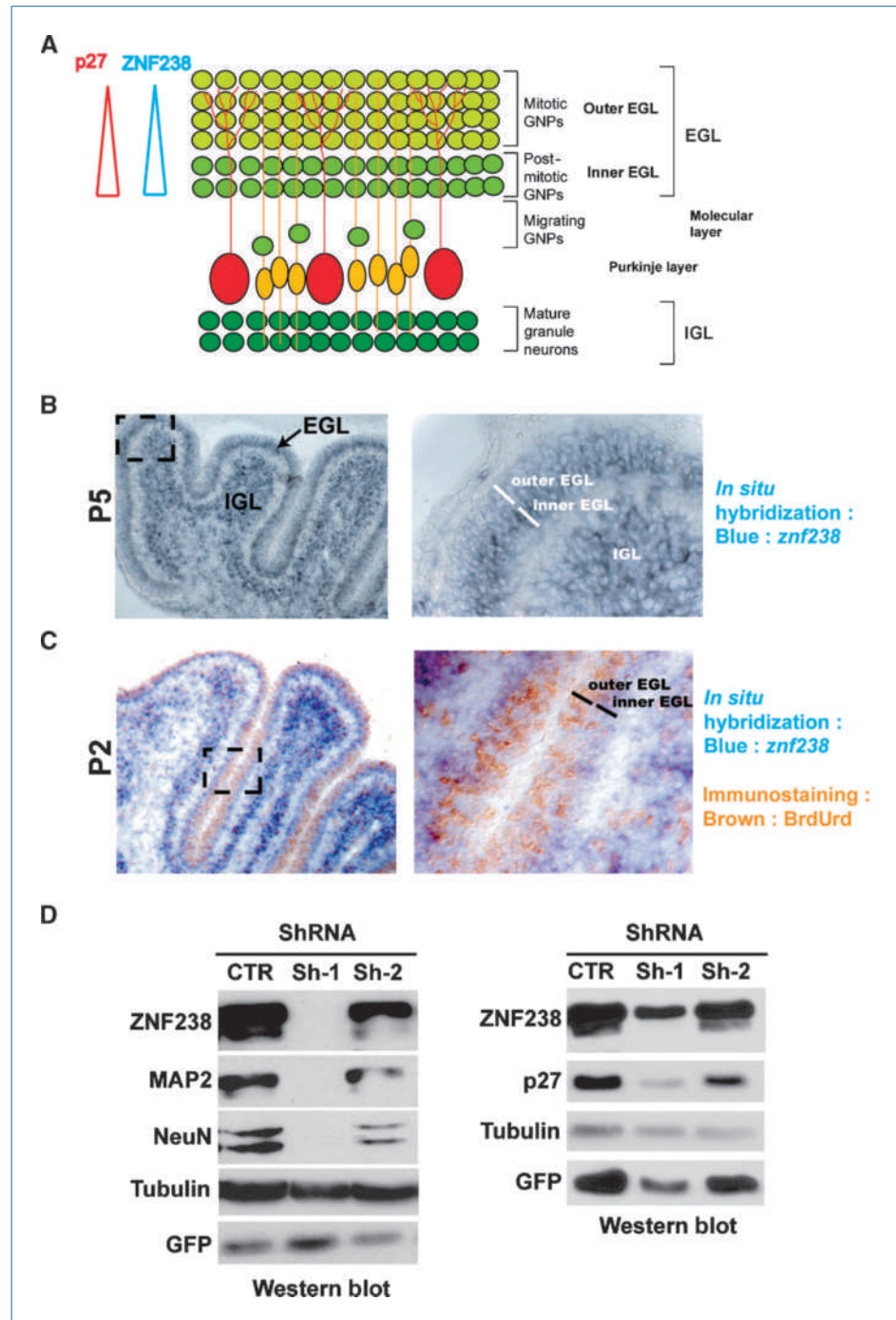
Note: Supplementary data for this article are available at Cancer Research Online (<http://cancerres.aacrjournals.org/>).

Corresponding Author: Nadia Dahmane, The Wistar Institute, 3601 Spruce Street, Philadelphia, PA 19104. Phone: 215-495-6840; Fax: 215-495-6832; E-mail: ndahmane@wistar.org.

doi: 10.1158/0008-5472.CAN-09-2249

©2010 American Association for Cancer Research.

Figure 1. ZNF238 is essential for GNP differentiation. A, schematic representation of the mouse cerebellar cortex in the first postnatal week (adapted from ref. 6 and Ruiz i Altaba et al., Nat Rev Neurosci 2002;3:24–33). Granule neurons (dark green), their precursors (light green), Purkinje neurons (red), and Bergmann glia (orange) are shown. GNPs proliferate in the outer EGL. Postmitotic GNPs accumulate in the inner EGL and migrate to the IGL through the molecular and Purkinje layers. Cycling GNPs in the outer EGL respond to SHH secreted by the Purkinje neurons by proliferating. During development, *znf238* and *p27* are expressed in a gradient increasing in cells as they leave the cell cycle and become post mitotic. B, *in situ* hybridization of *znf238* mRNA (blue) showing its expression in mouse cerebellum at P5. *Znf238* mRNA is expressed by GNPs as a gradient increasing from the outer to the inner part of the EGL and is highly expressed in the IGL. Right, high magnification of the left image. C, double labeling of *znf238* mRNA by *in situ* hybridization and BrdUrd as detected by immunohistochemistry. *Znf238* (blue) does not colocalize with BrdUrd (brown) in the EGL. Right, high magnification of the left image. D, Western blot showing a reduction in ZNF238 protein levels following shRNA expression in GNPs. Sh-1 and Sh-2 induce downregulation of ZNF238 expression, which triggers a decrease of MAP2, NeuN, and p27 expression. A shRNA targeting the expression of the luciferase enzyme was used as control (CTR).



protein SMOOTHENED (SMO), leading to the activation of transcription factors of the GLI family, which induce the expression of several genes that promote the proliferation of GNPs such as *cyclin D1* and *N-myc* (10, 11) as well as *Gli1* itself. In humans, mutations that constitutively activate the SHH pathway are found in about 25% of MBs (12). Moreover, heterozygous mice mutant for *Ptc1* develop spontaneous MBs (7, 13), a process that is enhanced by concomitant loss of *p53* (14).

However, in addition to the SHH pathway, the balance between proliferation and differentiation of the GNPs is also influenced by other signaling pathways including Notch (15) and bone morphogenetic proteins (16).

Despite all the information collected about the different mechanisms involved in normal and pathogenic development of the cerebellum, there are gaps in our knowledge on the mechanisms modulating GNP behavior that, when deregulated,

contribute to MB. For instance, it is not known how cycling GNP that receive mitogenic signals stop proliferating, become postmitotic, and begin to differentiate into mature neurons.

In the search for genes that could inhibit proliferation and enhance differentiation, we screened for the ones that were specifically expressed in postmitotic GNPs as well as granule neurons, but not in cycling GNPs.³ We identified a gene that fulfilled this criterion and that encodes the ZNF238 protein (17).

ZNF238 is a member of the BTB/POZ-ZF [Broad complex, Tramtrack, Bric à brac (BTB) or poxvirus and zing finger (POZ)-zinc finger] protein family, which contains several proteins involved in development and/or cancer formation, such as B-cell lymphoma 6 (BCL-6), promyelocytic leukemia zinc finger (PLZF), and hypermethylated in cancer 1 (HIC-1; ref. 18). The BTB/POZ domain of ZNF238 is located at its NH₂-terminal region and is highly conserved between human, mice, and zebrafish (Supplementary Fig. S1) whereas the four zinc fingers are located at the COOH-terminal part of the protein.

Additional reasons for our focus on ZNF238 came from its genomic location. Human *ZNF238* is located on chromosome 1q44 in a region that is deleted in patients with microcephaly (e.g., ref. 19), suggesting that it could play a role in coordinating the production of mature differentiated cells that form the bulk of the brain.

Here we show that ZNF238 is lost or very weakly expressed in MB and glioma cells and that its reinstatement results in compromised cell proliferation and tumor growth *in vivo*. Conversely, we show that knockdown of ZNF238 in GNPs leads to a reduction in their differentiation. Our results suggest that ZNF238 is a novel tumor suppressor that may be essential for the normal differentiation of neural precursors.

Materials and Methods

Plasmids and short hairpin RNAs

The full-length mouse *znf238* cDNA was PCR amplified from the EST BU701724. The PCR product was inserted in frame with 3Xflag tag in the vector p3Xflag-CMV-14 (Sigma), using *Bam*HI restriction sites. We have inserted the full-length mouse *znf238* cDNA in a lentiviral vector (pLSL; gift of Dr. P. Chumakov, Lerner Research Institute, The Cleveland Clinic Foundation, Cleveland, OH) in which a fragment containing IRES-green fluorescent protein (GFP), obtained following digestion of pIRES2-EGFP (Clontech) with *Xma*I-*Not*I, was inserted in the *Sal*I site of pLSL. The full-length *znf238* cDNA was also cloned into the TREAutoR3 plasmid (ref. 20; gift of Dr. D. Markusic, AMC Liver Center, Amsterdam, The Netherlands) after amplification using primers containing *Age*I and *Nsi*I restriction sites. The fragment was then digested with *Age*I and *Nsi*I and cloned into an *Age*I-*Pst*I digest of TREAutoR3.

We have used two short hairpin RNAs (shRNA) cloned in a lentiviral vector (PLL3.7; ref. 21) to knock down mouse *znf238*. One of these shRNAs targets a sequence located 715

nt from the start codon (Sh-1), whereas the second targets a sequence located in the 3'-untranslated region of the mRNA (Sh-2). We used a shRNA targeting a sequence located in the luciferase mRNA, as a control (21).

Western blots

Protein lysates were prepared in radioimmunoprecipitation assay buffer [50 mmol/L HEPES (pH 7.4), 0.5% sodium deoxycholate, 150 mmol/L NaCl, 1% NP40, 0.1% SDS] from cell lines or frozen tissues. Proteins were quantified using the bicinchoninic acid protein assay reagent (Thermo Scientific), resolved on SDS-PAGE, and transferred onto a polyvinylidene difluoride membrane (Millipore). The membrane was then incubated with the following antibodies: anti-ZNF238 (see Supplementary Fig. S2), anti-Flag (Sigma), anti-p27 (Santa Cruz), anti-cyclin D1 (Santa Cruz), anti-tubulin (Sigma), anti-GFP (Covance), anti-MAP2 (Sigma), and anti-NeuN (Chemicon).

GNP preparation and infection

Granule neuron precursor cultures were established as previously described (11, 16) with minor modifications. Cerebella from postnatal day 4 to 5 (P4–5) CD-1 mice were dissected in HBSS and the meninges were carefully removed. Cerebella were treated with trypsin (Sigma) and DNase I (Serlabo) for 20 min at 37°C and then triturated using fire-polished glass Pasteur pipettes. After centrifugation, the cell suspension was resuspended in DMEM/F-12 supplemented with glutamine (2 mmol/L), penicillin (50 units/mL), streptomycin (50 µg/mL), and B27 (1×, Life Technologies, Inc.) and passed through a cell strainer (Falcon). GNPs were then purified by depleting adherent cells with two rounds of 30-min plating on plastic dishes coated with poly-D-lysine (MP Biomedicals). The resulting cultures contain more than 95% granule cells. The cells were then pelleted and resuspended in DMEM/F-12 supplemented as described above and plated on poly-D-lysine-coated six-well plates at a density of 6 × 10⁶ per well. The following day, GNPs were infected with the different viruses for 6 h and proteins were isolated 4 d after infection.

In situ hybridization

In situ hybridization on sections was done as described previously, using digoxigenin-labeled RNA probes (22). *Znf238* digoxigenin-labeled antisense riboprobe was generated from linearized plasmids encoding full-length mouse *znf238*.

Bromodeoxyuridine immunostaining

Tissues or cells were fixed with 4% paraformaldehyde and treated for 30 min with 2 N HCl followed by a 20-min wash in sodium borate (Borax) buffer (pH 8.5). Incubation with bromodeoxyuridine (BrdUrd) antibody solution was carried out overnight at 4°C (1:400; Becton Dickinson). Sections or cells were then incubated for 1 h at room temperature with secondary antibody and mounted in mounting medium.

Tumor cell line cultures

Human tumor cell lines (U87MG, U251, D283, D341, and DAOY) were obtained from the American Type Culture Collection. Mouse medulloblastoma cell lines derived from *Ptch1*^{+/-}

³ N. Dahmane and A. Ruiz i Altaba, unpublished data.

or *Ptch1*^{+/-};*p53*^{-/-} medulloblastoma (14) were kindly provided by Dr. T. Curran (Children's Hospital of Philadelphia, Philadelphia, PA). All cell lines were cultured in DMEM (Life Technologies, Inc.) supplemented with 10% fetal bovine serum (Hyclone).

Colony formation assays

DAOY and U251 cell lines were transfected using Lipofectamine 2000 (Sigma) for 6 h with either ZNF238-Flag or empty vector as control. G418 (600 µg/mL; Sigma) was added for selection of transfected cells for 48 h. Then, 3×10^4 (U251) or 1×10^4 (DAOY) cells were plated per 60-mm dish. The cells were grown to form colonies in medium supplemented with G418 (600 µg/mL) for 1 mo, then were fixed with 100% methanol and stained in a solution of 0.5% methylene blue/70% isopropanol. This experiment was done three times in duplicate for each cell line. U87MG cells were infected overnight with the same titer of ZNF238-IRES-GFP- or GFP-expressing lentiviruses in regular medium supplemented with 10 µg/mL polybrene. Three days after transduction, the percentage of transduced cells was determined by fluorescence-activated cell sorting (FACS) analysis. Only samples with a percentage of transduced cells higher than 95% were used for the colony formation assays. Transduced cells were diluted to 1,000 cells per 60-mm plate. On the day of plating, each sample was analyzed by Western blot to verify the expression of ZNF238 protein. One month after plating the cells, GFP expression was verified using a fluorescent microscope and colonies were fixed and stained as described above. This experiment was done two times in quadruplicate.

U87MG cells stably expressing tetracycline-inducible ZNF238 protein were generated and used for the colony forming assays. Cells were plated at a density of 100 per well in a six-well plate. Twenty-four hours after plating, doxycycline or carrier was added to cultured cells. The cells were grown for 3 wk, and formed colonies were fixed and stained as described above. This experiment was done twice in triplicate.

Cell proliferation assay

U87MG and DAOY cells stably expressing doxycycline-inducible ZNF238 were used for BrdUrd incorporation. U87MG and DAOY cells were plated onto poly-D-lysine-coated coverslips and treated for 2 d with 10 µg/mL doxycycline. On the second day, a 5- or 15-min pulse of BrdUrd (100 µg/mL) was applied to the DAOY or U87MG cells, respectively. The cells were then fixed and immunostained.

Apoptosis

DAOY cells stably expressing doxycycline-inducible ZNF238 were plated on poly-D-lysine-coated coverslips at a density of 2×10^4 per well. The following day, cells were treated with 10 µg/mL doxycycline or vehicle. Cells were fixed with 4% paraformaldehyde 48 h after treatment and stained for cleaved caspase-3 (cleaved caspase-3 antibody, 1/100, Cell Signaling). The cells were then incubated with the secondary antibody coupled with FITC and the nuclei were counterstained with Hoechst. Pictures were taken at $\times 20$ magnification and 10 fields per coverslip were counted in duplicate in

two independent experiments. The *t* test was used for statistical analysis.

Western blot analysis of cleaved caspase-3 expression. U87MG cells stably expressing doxycycline-inducible ZNF238 were also plated on 10-cm dishes and treated with doxycycline. DAOY cells were plated on 10-cm dishes and transfected with empty vector (control) or ZNF238-Flag. Three days after addition of doxycycline (U87) or cell transfection (DAOY), proteins were extracted and the expression of cleaved caspase-3 was analyzed by Western blot.

RNA analysis

RNAs were purified using Trizol from U87MG and DAOY cells stably expressing doxycycline-inducible ZNF238, 3 d after treatment with doxycycline (10 µg/mL). Quantitative reverse transcription-PCR (RT-PCR) was done using the following primers: p27-F, 5'-CCGGCTAACTCTGAGGACAC-3'; p27-R, 5'-AGAAGAATCGTCCGGTTGCAG-3' (23); β -actin-F, 5'-CTCCTCCTGAGCGCAAGTACTC-3'; β -actin-R, 5'-CAT-CTCCTGCTTGCTGATCCA-3' (24); cyclin D1-F, 5'-CTGGAGGTCTGCGAGGAACA-3'; cyclin D1-R, 5'-CCTTCATCTTAGAGGCCACGAA-3' (24).

Xenograft experiments

U251, U87MG, and DAOY cells were transduced with lentiviruses expressing GFP only or ZNF238-IRES-GFP overnight with 10 µg/mL polybrene. Two days after transduction, the percentage of infected cells was determined by FACS analysis (GFP expression), and the ectopic ZNF238 expression in cells analyzed by Western blot. Three million U251 cells in 100 µL of PBS were then injected s.c. on the back of nude mice (Taconic), and 1×10^6 DAOY cells as well as 2×10^6 U87MG cells were resuspended in a mix of 1:1 PBS/Matrigel followed by s.c. injection in the back of nonobese diabetic/severe combined immunodeficient mice (Taconic).

Statistical analysis

Unless otherwise noted, all statistical analyses were done using the Mann-Whitney test.

Results

ZNF238 is differentially expressed by cerebellar granule neuron precursors and localizes to the postmitotic population. ZNF238 was isolated from a differential hybridization screen followed by an *in situ* hybridization expression screen in the brain⁴ using similar methods to already described expression screens (25). We sought to carefully determine the localization of its expression in relation to the pool of cycling GNP in the cerebellum. During the first 2 to 3 weeks after birth, the mouse cerebellar cortex is formed by four main layers: the EGL, the molecular layer, the Purkinje layer, and the IGL. The EGL is itself composed of two layers: the outer EGL, containing the proliferating GNPs, and the inner EGL, containing the newly postmitotic GNPs that begin to

⁴ N. Dahmane, unpublished data.

differentiate as neurons and migrate inward. *Znf238* mRNA was found to be expressed in a graded fashion in the EGL (low in the outer EGL and high in the inner EGL) and also strongly expressed in the IGL (Fig. 1B and C). *In situ* hybridization analyses were then done to detect both *znf238* mRNA expression and BrdUrd immunostaining at P2 following a 2-hour BrdUrd pulse. As expected, proliferating BrdUrd-positive cells were mainly localized in the outer EGL. Double *in situ* and BrdUrd analyses showed that *znf238*⁺ cells in the inner EGL are not BrdUrd⁺ and that BrdUrd⁺ cells in the outer EGL are not *znf238*⁺ (Fig. 1C). ZNF238 is thus exclusively expressed at high levels in postmitotic GNP.

Knockdown of ZNF238 compromises neuronal differentiation in purified GNPs. The pattern of expression of *znf238* mRNA in the cerebellar cortex suggests that it could be involved in the differentiation of granule neurons from postmitotic GNPs. To begin to address this possibility, we purified P5 mouse GNPs and investigated ZNF238 function in these cells through RNA interference using shRNA-expressing, replication-incompetent lentiviral vectors. Purified GNPs briefly proliferate *in vitro* before starting to differentiate as granule neurons (e.g., ref. 26). We used two different shRNAs, shRNA-1 and shRNA-2, designed to target two different sequences within *Znf238*. ZNF238 expression was assessed using a polyclonal antibody that we developed in rabbit against the COOH-terminal part of the protein. The characterization of this antibody was carried out using HEK293T cells stably expressing ZNF238 with a Flag tag at the COOH-terminal part of the protein. Both the Flag and the ZNF238 antibodies recognize the ZNF238 protein (Supplementary Fig. S2A), known to migrate between 64 and 82 kDa (17). The protein runs as a doublet, the slower one corresponding to a phosphorylated form (Supplementary Fig. S2B). Both shRNA-1 and shRNA-2 downregulated ZNF238 protein expression levels, whereas tubulin levels were unmodified (Fig. 1D).

We found that ZNF238 knockdown leads to a strong reduction or the loss of expression of the neuronal markers MAP2 and NeuN, as well as to a downregulation of the p27

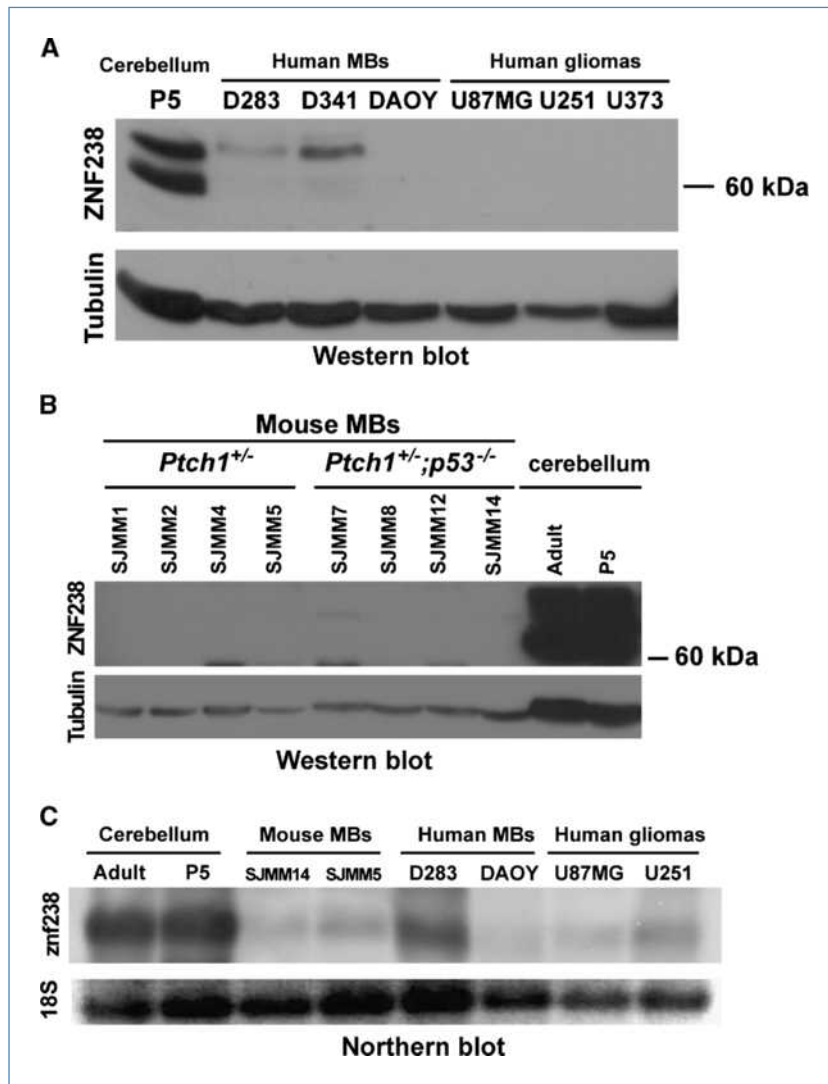
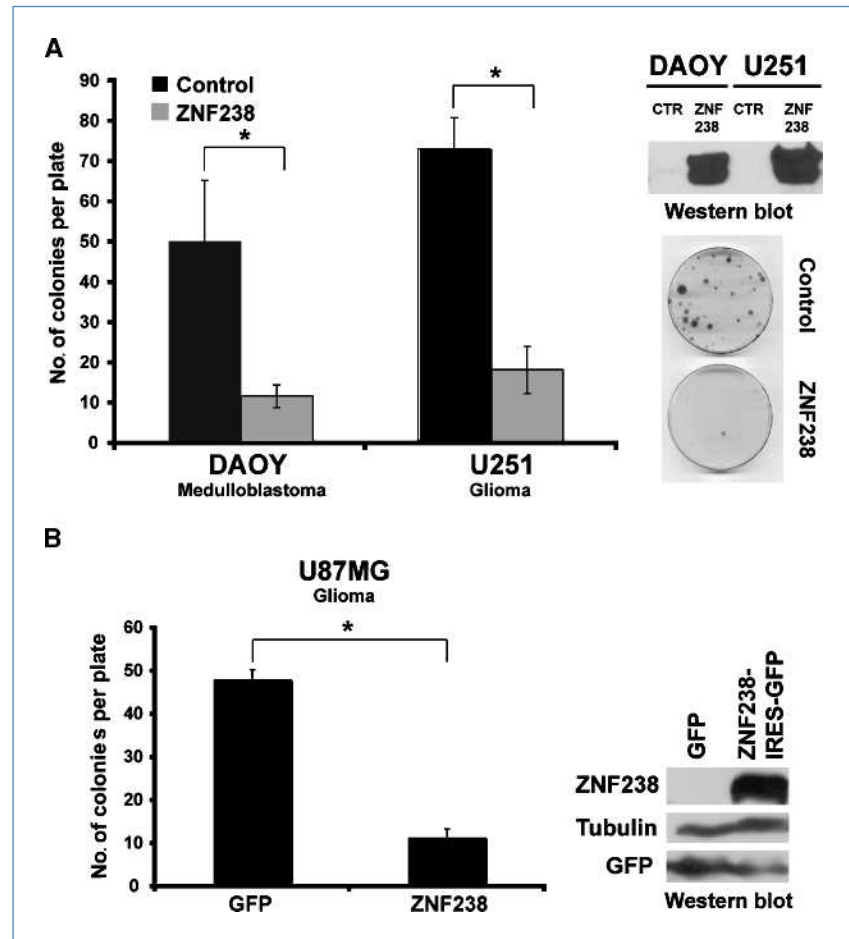


Figure 2. Brain tumor cell lines lack or express low levels of ZNF238 protein. A and B, Western blots showing the expression levels of ZNF238 protein in brain tumor cell lines. A, ZNF238 expression is very low in human MB cell lines D283 and D341 and not detected in DAOY cells as well as the human glioma cell lines U87MG, U251, and U373. Mouse P5 cerebellum is used as positive control. B, ZNF238 protein is not expressed in mouse MB cell lines derived from *Ptch1*^{+/-} and *Ptch1*^{+/-}; *p53*^{-/-} mice, whereas it is normally expressed in adult and P5 mouse cerebellum. C, Northern blot showing a downregulation of *znf238* mRNA in tumor cell lines when compared with control tissues. Pictures of the gel showing 18S RNA were taken before and after transfer to ensure that the same amount of RNA was loaded and transferred on the membrane.

Figure 3. ZNF238 expression suppresses brain tumor cell colony formation. A, histograms showing the quantification of colonies formed by the MB (DAOY) and glioma (U251) cell lines transfected with either empty vector (CTR) or ZNF238-Flag. ZNF238 expression decreases the ability of the tumor cell lines to form colonies by approximately five times, as shown in the graph (left) and illustrated in the picture of the colonies (right). B, GFP-expressing U87MG cells form higher number of colonies when compared with ZNF238-IRES-GFP-expressing U87MG cells.



protein, a major regulator of differentiation and cell cycle progress of GNP (27).

These knockdown experiments suggest that ZNF238 is required for normal GNP differentiation and that it may be involved in GNP cell cycle exit and proliferation arrest. Whereas studies with transgenic mice are in progress and support this notion,⁵ these results prompted us to examine the expression of ZNF238 in brain tumors, including MBs.

ZNF238 expression is low or absent in brain tumor cells. We first analyzed the expression of ZNF238 protein in human and mouse MB cells. Cerebellum tissues from P5 and adult mice were used as positive controls because P5 mouse cerebellum has been shown to present a similar transcription profile as human MBs (28). The expression of ZNF238 protein was found to be very low in D283 and D341 and absent in DAOY human MB cells (Fig. 2A). Moreover, we also tested ZNF238 expression in mouse cell lines derived from *Ptch1*^{+/-} and *Ptch1*^{+/-};*p53*^{-/-} MBs (14, 29) and observed that none expressed ZNF238 when compared with P5 and adult cerebellum (Fig. 2B). Interestingly, ZNF238 protein also

seemed to be absent in human GBM U87MG, U343, and U251 cells (Fig. 2A).

Because ZNF238 protein levels are strongly decreased or absent in tumor cells, we examined *znf238* mRNA expression by Northern blot to test if the downregulation was primarily at the mRNA or protein level. High levels of *znf238* mRNA were present in control tissues (adult and P5 cerebellum) compared with the much lower levels of expression observed in tumor cells (Fig. 2C). Levels of *znf238* mRNA expression in mouse MB cells were also much lower than those observed in mouse P5 cerebellum and were comparable to the levels observed in human brain tumor cells (Fig. 2C), suggesting that ZNF238 expression is deregulated in brain tumor cells at the transcriptional level.

ZNF238 inhibits brain tumor cell proliferation in vitro. The results presented above show that brain tumor cells display low or no ZNF238 expression, suggesting that this is a requisite for tumor development. We thus tested if reinstated or enhanced ZNF238 expression may negatively affect the growth of brain tumors. Using plasmid transfection or lentiviral vectors (see Materials and Methods), full-length ZNF238 was constitutively or conditionally expressed in DAOY, U87MG, and U251 cells, and the effect of its expression on the ability of these tumor cells to form colonies *in vitro* was tested.

⁵ Xiang et al., in preparation.

For each cell line, we observed that ZNF238 expression reduced the potential of tumor cells to form colonies *in vitro* at 3 weeks after plating and following methylene blue staining (Fig. 3; Supplementary Fig. S3). DAOY and U87MG cells expressing ZNF238 showed 1/5th whereas U251 cells expressing cells showed 1/8th the number of colonies as compared with control cells (Fig. 3).

ZNF238 antagonizes brain tumor growth *in vivo*. To examine the possible similar action of ZNF238 *in vivo*, brain tumor cells expressing ZNF238 were implanted s.c. in immunodeficient mice and tumor development was monitored over 4 to 8 weeks (Fig. 4). For each experiment, five

mice each were used in the control and ZNF238 groups for each cell type. Four of five mice developed tumors when implanted with U251 control cells (U251^{Control}) at 4 weeks (mean diameter, 3.8 ± 1.4 mm) and the tumor size increased up to 8 weeks when the mice were sacrificed (mean diameter, 7.9 ± 1.6 mm). In contrast, U251 cells expressing ZNF238 (U251^{ZNF238}) failed to form any tumors at all at 4 or 8 weeks (Fig. 4A), suggesting a very potent tumor inhibitory role *in vivo*.

In U87MG and DAOY cells, ZNF238 also had inhibitory effects, although these were milder (Fig. 4B and C). At 4 weeks, the volume of the tumor formed by U87MG^{ZNF238} and DAOY^{ZNF238} cells was dramatically reduced as compared

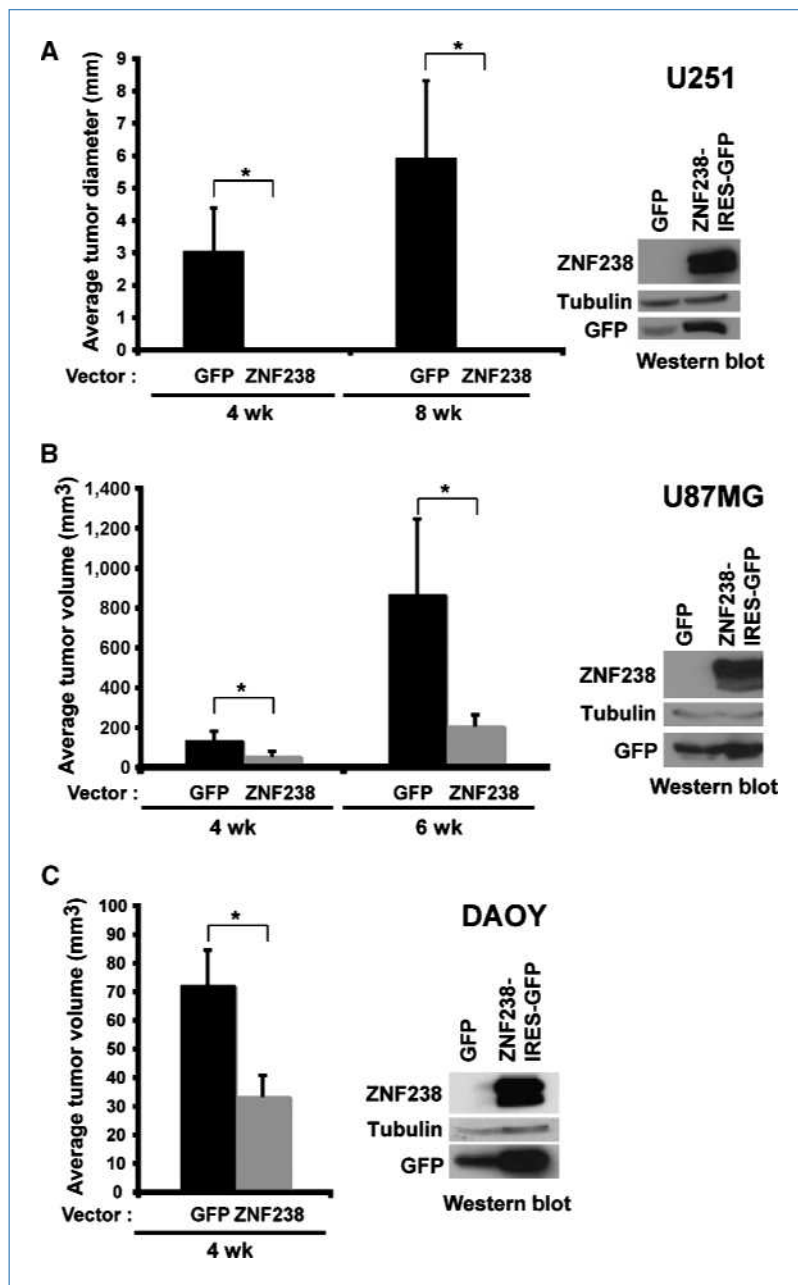
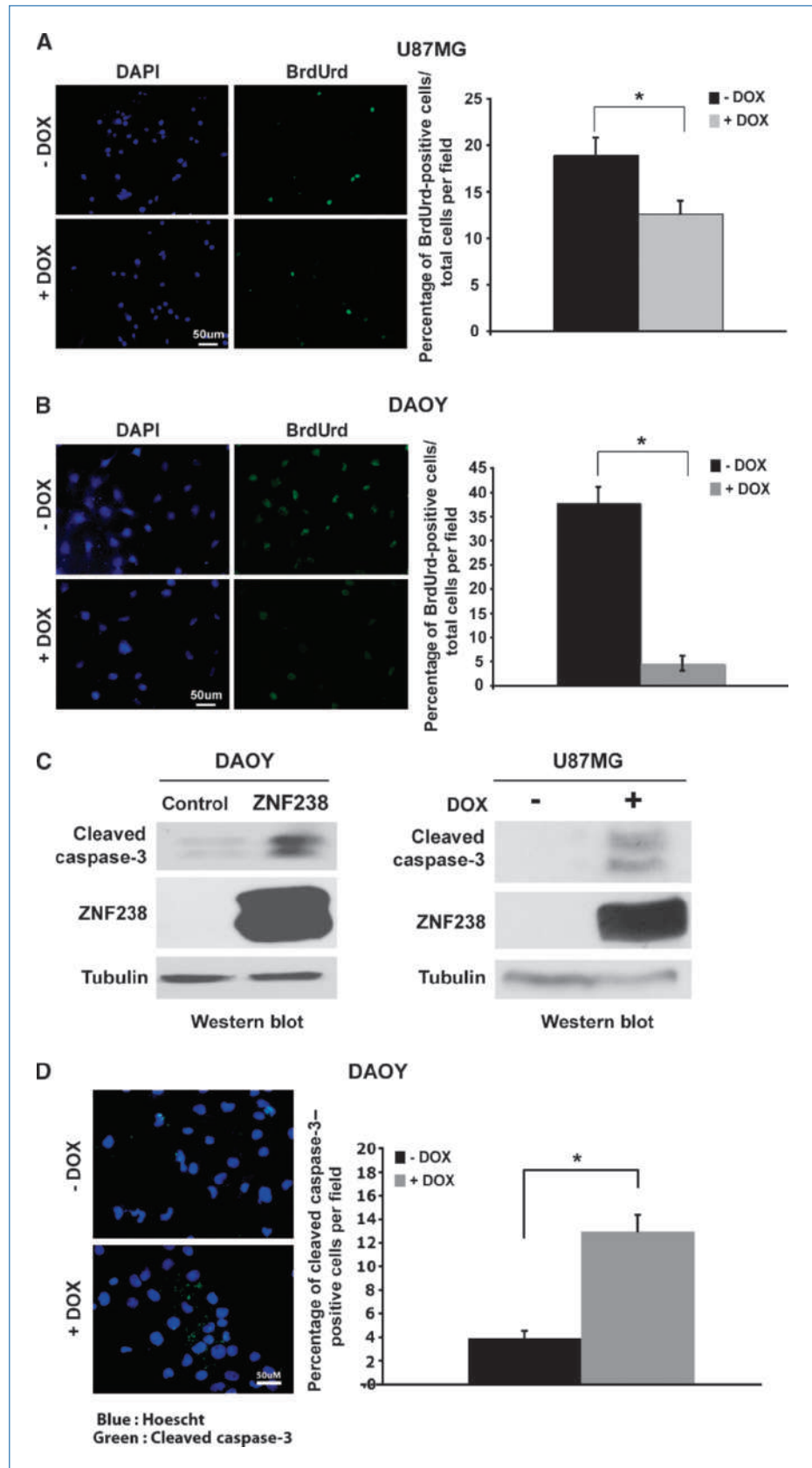


Figure 4. ZNF238 dramatically decreases growth of brain tumor xenografts *in vivo*. A to C, histograms showing the quantification of diameter (A) and volume (B and C) of brain tumor xenografts. The Western blots on the right side of each histogram show the levels of expression of ZNF238 in cells used for the xenograft assays.

A, ZNF238-expressing U251 cells do not form tumors in nude mice after either 4 or 8 wk as compared with control GFP-expressing cells. B, 6 wk after implantation, the average tumor volume of GFP-expressing U87MG cells is dramatically higher as compared with the average tumor volume of ZNF238-expressing cells. C, 4 wk after implantation, the volume of tumors formed by ZNF238-expressing DAOY cells is ~2-fold smaller than the volume of tumor developed from GFP-expressing DAOY cells.

Figure 5. ZNF238 decreases tumor cell proliferation and induces an increase of apoptosis of tumor cells. A and B, U87MG (A) and DAOY (B) cell lines, stably transduced to express ZNF238 under the control of doxycycline (DOX), were incubated with BrdUrd for 15 or 30 min, respectively. Left, ZNF238 expression decreases cell proliferation as shown by BrdUrd immunostaining. Right, quantification of the percentage of BrdUrd⁺ cells per field following expression of ZNF238 in U87MG and DAOY cells. C, Western blots were done on proteins extracted from DAOY (A) and U87MG (B). DAOY cells were transfected with empty vector (control) or ZNF238-Flag. U87MG cells stably expressing doxycycline-inducible ZNF238 were treated with vehicle or doxycycline. Induction of ZNF238 expression induces an increase of cleaved caspase-3 expression. D, DAOY cells stably expressing doxycycline-inducible ZNF238 cells were treated with vehicle or doxycycline, and expression of cleaved-caspase-3 was analyzed by immunocytochemistry. Cleaved caspase-3 is shown in green and cell nuclei, stained with Hoechst stain, are shown in blue (left). Pictures were taken at $\times 20$ magnification and the percentage of cleaved-caspase-3-positive cells per field was counted. Quantification is shown in the left panel. Right, increase of apoptosis of the doxycycline-treated cells is statistically significant when compared with the vehicle-treated cells ($P < 0.001$; right).



with control cells (U87MG^{Control}: 141.9 ± 43.7 mm³, versus U87MG^{ZNF238}: 65.2 ± 11.7 mm³; DAOY^{Control}: 72.7 ± 12.04 mm³, versus DAOY^{ZNF238}: 34.0 ± 7.1 mm³; $P < 0.05$ for both cell types). However, the difference in tumor volume between DAOY^{Control} and DAOY^{ZNF238} tumors was no longer significant at 6 weeks (not shown), whereas it still persisted for U87MG tumors (U87MG^{Control}: 873.3 ± 378 mm³, versus U87MG^{ZNF238}: 216.6 ± 51.2; $P < 0.05$). This was found to result from the loss of exogenous ZNF238 expression in DAOY^{ZNF238}, indicating that the effect is reversible. Although the mechanism for this suppression remains to be determined, the results highlight the ability of ZNF238 to inhibit human brain tumor cell proliferation as well as tumor growth *in vivo*.

ZNF238 decreases cell proliferation and promotes cell death. To begin to investigate the mechanisms involved in the blockade of brain tumor growth by ZNF238, we examined whether it might reduce cell proliferation and/or increase cell death. We used U87MG or DAOY clones stably transduced to express ZNF238 using the tetracycline-inducible system (e.g., ref. 30). U87MG^{ZNF238} and DAOY^{ZNF238} cells showed ~30% (Fig. 5A) and ~87% (Fig. 5B) decreases in the rate of proliferation as measured by BrdUrd incorporation when compared with U87MG^{Control} and DAOY^{Control} cells, respectively. In addition to an inhibition of cell proliferation, ZNF238 expression provoked an important increase

in apoptosis as shown by Western blot and immunohistochemistry of cleaved caspase-3 (Fig. 5C and D).

ZNF238 acts on key cell cycle regulators. To delineate the mechanism by which ZNF238 negatively affects cell growth, we determined the expression of the key cell cycle regulators, cyclin D1 and p27. Cyclin D1 is the main G₁-promoting cyclin and p27 is a key cyclin-dependent kinase inhibitor, and both have been shown to be important for GNP development (27, 31). ZNF238 knockdown in purified GNPs induced a strong decrease of p27 protein expression (Fig. 1D). Conversely, p27 protein levels in MB and glioma cells with reinstated ZNF238 expression were strongly upregulated when compared with control cells (Fig. 6). Concomitant with the increase of p27 protein levels, ZNF238 sharply decreased cyclin D1 protein expression (Fig. 6A and B). These results suggest that ZNF238 may inhibit tumor development via the control of key cell cycle regulators such as cyclin D1 and p27. Moreover, as shown by RT-PCR and quantitative RT-PCR analyses, the changes in p27 and cyclin D1 protein levels are correlated with changes in RNA expression (Fig. 6C and D). These results suggest that ZNF238 regulates those genes, at least in part, at the transcriptional level.

ZNF238 promotes aspects of neuronal differentiation in brain tumor cells. Cell cycle arrest can lead to different events such as quiescence, cell death, or cell differentiation in a context-dependent manner. Because ZNF238 is

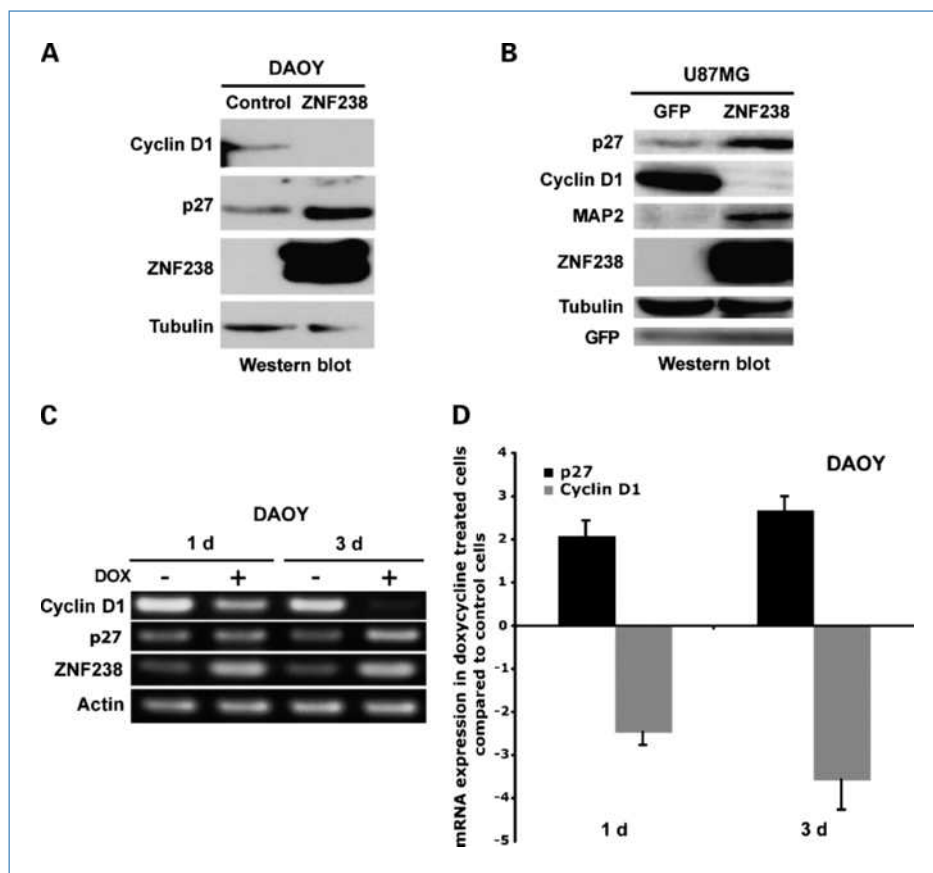


Figure 6. ZNF238 regulates p27 and cyclin D1 expression. A and B, DAOY cells stably expressing doxycycline-inducible ZNF238 (A) and U87MG cells transduced to express either GFP as control or ZNF238-IRES-GFP (B) were used. The Western blots show that ZNF238 expression in DAOY cells (A) and U87MG cells (B) induces a significant decrease of cyclin D1 protein levels as well as an increase in p27 expression. An increase in MAP2 protein levels is also observed when U87MG cells express ZNF238 compared with control cells (B). C and D, RNAs were extracted from DAOY cells stably expressing doxycycline-inducible ZNF238, 1 and 3 d after treatment with vehicle or doxycycline, and quantitative PCR was done. RT-PCR (C) shows that ZNF238 expression induces a decrease of cyclin D1 mRNA as well as an increase of p27 mRNA expression. These results are quantified by quantitative RT-PCR (D).

expressed in GNP as they exit the cell cycle and start their differentiation, we investigated whether it may suppress tumor development by arresting their proliferation, possibly trying to promote their differentiation. We found that re-stored ZNF238 in brain tumor cells induced higher levels of the bona fide neuronal differentiation marker MAP2 in U87MG glioma cells (Fig. 6B), supporting the idea that ZNF238 may act to induce cell differentiation, involving the cessation of proliferation. However, brain tumor cells may not be able to yield normal differentiated neurons, and the block imposed by ZNF238 may instead lead to abortive differentiation and cell death.

Discussion

The growth of individual organs is under the strict control of mechanisms that can measure final size and, likely, cell numbers. During embryogenesis and in early postnatal stages, the brain primordia undergo massive growth, and a number of growth factors have been described to be critical for this process. For example, SHH signaling plays an important role in the growth of the cerebellum, where it controls the proliferation of GNP in the EGL and the differentiation of Bergmann glial cells (6). Similarly, it controls the proliferation of neural precursors in the cortex and tectum (32) and of neural stem cells (33–36). However, what is not clear is how cells perceive a stop signal to cease proliferation, and thus organ growth, and begin to differentiate in an orderly manner to create the appropriate cell types in appropriate numbers. In the case of the cerebellum, for instance, it is not known how the proliferating GNP in the outer EGL become postmitotic and begin to differentiate as granule neurons that will form the IGL.

Here we have investigated the possible role of ZNF238 as a pro-differentiation and antiproliferative factor in the cerebellum and in brain tumors. We report that ZNF238 is preferentially expressed at high levels in nonproliferating GNP and in differentiated granule neurons in the IGL. Its expression is very low in mitotically active GNP. ZNF238 is also expressed in other brain precursor populations such as intermediate neuronal progenitors in the cerebral cortex (37).

Loss-of-function analyses with RNA interference show a participation of ZNF238 in the control of GNP differentiation: ZNF238 is essential for the expression of p27, a key cell cycle inhibitor important for GNP cell cycle exit (27). Moreover, ZNF238 knockdown decreases the expression of neuronal differentiation markers in cultured GNP. The functional results

with purified normal GNP and the localization of the expression of ZNF238 allow us to suggest that it functions to counteract pro-proliferative mechanisms that maintain GNP cycling in the outer EGL.

Importantly, we find that human and mouse MBs and GBMs lack ZNF238 expression or harbor very low levels. We find that reinstated ZNF238 function (or enhanced function in the case of cells that express very low levels) in human brain tumor cells inhibits their proliferation *in vitro* and tumor growth *in vivo*. This is highly significant, as it seems that human brain tumor cells must downregulate ZNF238 to proliferate. Thus, the inhibition of tumor growth or the great decrease in tumor volume in xenografts that we observe indicates that ZNF238 acts as a novel brain tumor suppressor.

Because many MBs are thought to arise from GNP, the suppression of ZNF238 in cerebellar GNP would allow these cells to maintain an active proliferative state similar to that of GNP in the outer EGL. Indeed, the transcriptional profile of MBs is most similar to that of GNP at P5, a time of peak GNP proliferation (28).

How ZNF238 may interact with the SHH, insulin-like growth factor, or other mitogenic pathways that affect GNP remains to be determined. Nevertheless, our results highlight the parallel between development and cancer and point to the reactivation of ZNF238 expression or its enhancement as possible therapeutic avenues for certain brain tumors that are incurable to date.

Disclosure of Potential Conflicts of Interest

No potential conflicts of interest were disclosed.

Acknowledgments

We thank L. Holderbaum for excellent technical assistance in cloning ZNF238 in the AutoR3 plasmid; V. Baubet, R. Desmarest, F. Rauscher III, and A. Ruiz i Altaba for discussions and comments on the manuscript; and T. Curran, D. Markusik, and P. Chumakov for reagents.

Grant Support

The A. Taxin Brain Cancer Center at the Wistar Institute, the WW Smith Charitable Trust, the V Foundation, the National Brain Tumor Society, and the American Cancer Society to N. Dahmane, as well as from the Wistar Cancer Center Support grant NIH CA010815.

The costs of publication of this article were defrayed in part by the payment of page charges. This article must therefore be hereby marked *advertisement* in accordance with 18 U.S.C. Section 1734 solely to indicate this fact.

Received 6/23/09; revised 10/28/09; accepted 11/10/09; published OnlineFirst 1/26/10.

References

1. Ellison D. Classifying the medulloblastoma: insights from morphology and molecular genetics. *Neuropathol Appl Neurobiol* 2002;28:257–82.
2. Gilbertson RJ. Medulloblastoma: signalling a change in treatment. *Lancet Oncol* 2004;5:209–18.
3. Goldowitz D, Hamre K. The cells and molecules that make a cerebellum. *Trends Neurosci* 1998;21:375–82.
4. Sotelo C. Cellular and genetic regulation of the development of the cerebellar system. *Prog Neurobiol* 2004;72:295–339.
5. Wang VY, Zoghbi HY. Genetic regulation of cerebellar development. *Nat Rev Neurosci* 2001;2:484–91.
6. Dahmane N, Ruiz i Altaba A. Sonic hedgehog regulates the growth and patterning of the cerebellum. *Development* 1999;126:3089–100.
7. Lewis PM, Gritti-Linde A, Smeyne R, Kottmann A, McMahon AP. Sonic hedgehog signaling is required for expansion of granule neuron precursors and patterning of the mouse cerebellum. *Dev Biol* 2004;270:393–410.
8. Wallace VA. Purkinje-cell-derived Sonic hedgehog regulates granule

- neuron precursor cell proliferation in the developing mouse cerebellum. *Curr Biol* 1999;9:445–8.
9. Wechsler-Reya RJ, Scott MP. Control of neuronal precursor proliferation in the cerebellum by Sonic Hedgehog. *Neuron* 1999;22:103–14.
 10. Kenney AM, Cole MD, Rowitch DH. Nmyc upregulation by sonic hedgehog signaling promotes proliferation in developing cerebellar granule neuron precursors. *Development* 2003;130:15–28.
 11. Kenney AM, Rowitch DH. Sonic hedgehog promotes G(1) cyclin expression and sustained cell cycle progression in mammalian neuronal precursors. *Mol Cell Biol* 2000;20:9055–67.
 12. Marino S. Medulloblastoma: developmental mechanisms out of control. *Trends Mol Med* 2005;11:17–22.
 13. Goodrich LV, Milenkovic L, Higgins KM, Scott MP. Altered neural cell fates and medulloblastoma in mouse patched mutants. *Science* 1997;277:1109–13.
 14. Wetmore C, Eberhart DE, Curran T. Loss of p53 but not ARF accelerates medulloblastoma in mice heterozygous for patched. *Cancer Res* 2001;61:513–6.
 15. Solecki DJ, Liu XL, Tomoda T, Fang Y, Hatten ME. Activated Notch2 signaling inhibits differentiation of cerebellar granule neuron precursors by maintaining proliferation. *Neuron* 2001;31:557–68.
 16. Rios I, Alvarez-Rodriguez R, Marti E, Pons S. Bmp2 antagonizes sonic hedgehog-mediated proliferation of cerebellar granule neurons through Smad5 signalling. *Development* 2004;131:3159–68.
 17. Aoki K, Meng G, Suzuki K, et al. RP58 associates with condensed chromatin and mediates a sequence-specific transcriptional repression. *J Biol Chem* 1998;273:26698–704.
 18. Kelly KF, Daniel JM. POZ for effect-POZ-ZF transcription factors in cancer and development. *Trends Cell Biol* 2006;16:578–87.
 19. Hill AD, Chang BS, Hill RS, et al. A 2-Mb critical region implicated in the microcephaly associated with terminal 1q deletion syndrome. *Am J Med Genet* 2007;143A:1692–8.
 20. Markusic D, Oude-Elferink R, Das AT, Berkhout B, Seppen J. Comparison of single regulated lentiviral vectors with rTA expression driven by an autoregulatory loop or a constitutive promoter. *Nucleic Acids Res* 2005;33:e63.
 21. Rubinson DA, Dillon CP, Kwiatkowski AV, et al. A lentivirus-based system to functionally silence genes in primary mammalian cells, stem cells and transgenic mice by RNA interference. *Nat Genet* 2003;33:401–6.
 22. Tiveron MC, Hirsch MR, Brunet JF. The expression pattern of the transcription factor Phox2 delineates synaptic pathways of the autonomic nervous system. *J Neurosci* 1996;16:7649–60.
 23. Acosta JC, Ferrandiz N, Bretones G, et al. Myc inhibits p27-induced erythroid differentiation of leukemia cells by repressing erythroid master genes without reversing p27-mediated cell cycle arrest. *Mol Cell Biol* 2008;28:7286–95.
 24. Card DA, Hebbar PB, Li L, et al. Oct4/Sox2-regulated miR-302 targets cyclin D1 in human embryonic stem cells. *Mol Cell Biol* 2008;28:6426–38.
 25. Gitton Y, Dahmane N, Baik S, et al. A gene expression map of human chromosome 21 orthologues in the mouse. *Nature* 2002;420:586–90.
 26. Gao WO, Heintz N, Hatten ME. Cerebellar granule cell neurogenesis is regulated by cell-cell interactions *in vitro*. *Neuron* 1991;6:705–15.
 27. Miyazawa K, Himi T, Garcia V, Yamagishi H, Sato S, Ishizaki Y. A role for p27/Kip1 in the control of cerebellar granule cell precursor proliferation. *J Neurosci* 2000;20:5756–63.
 28. Kho AT, Zhao Q, Cai Z, et al. Conserved mechanisms across development and tumorigenesis revealed by a mouse development perspective of human cancers. *Genes Dev* 2004;18:629–40.
 29. Sasai K, Romer JT, Lee Y, et al. Shh pathway activity is down-regulated in cultured medulloblastoma cells: implications for preclinical studies. *Cancer Res* 2006;66:4215–22.
 30. Gossen M, Bujard H. Efficacy of tetracycline-controlled gene expression is influenced by cell type: commentary. *BioTechniques* 1995;19:213–6, discussion 6–7.
 31. Pogoriler J, Millen K, Utset M, Du W. Loss of cyclin D1 impairs cerebellar development and suppresses medulloblastoma formation. *Development* 2006;133:3929–37.
 32. Dahmane N, Sanchez P, Gitton Y, et al. The Sonic Hedgehog-Gli pathway regulates dorsal brain growth and tumorigenesis. *Development* 2001;128:5201–12.
 33. Palma V, Lim DA, Dahmane N, et al. Sonic hedgehog controls stem cell behavior in the postnatal and adult brain. *Development* 2005;132:335–44.
 34. Palma V, Ruiz i Altaba A. Hedgehog-GLI signaling regulates the behavior of cells with stem cell properties in the developing neocortex. *Development* 2004;131:337–45.
 35. Ahn S, Joyner AL. *In vivo* analysis of quiescent adult neural stem cells responding to Sonic hedgehog. *Nature* 2005;437:894–7.
 36. Machold R, Hayashi S, Rutlin M, et al. Sonic hedgehog is required for progenitor cell maintenance in telencephalic stem cell niches. *Neuron* 2003;39:937–50.
 37. Ohtaka-Maruyama C, Miwa A, Kawano H, Kasai M, Okado H. Spatial and temporal expression of RP58, a novel zinc finger transcriptional repressor, in mouse brain. *J Comp Neurol* 2007;502:1098–108.

Cancer Research

The Journal of Cancer Research (1916–1930) | The American Journal of Cancer (1931–1940)

ZNF238 Is Expressed in Postmitotic Brain Cells and Inhibits Brain Tumor Growth

Valérie M. Tatard, Chaomei Xiang, Jaclyn A. Biegel, et al.

Cancer Res 2010;70:1236-1246. Published OnlineFirst January 26, 2010.

Updated version	Access the most recent version of this article at: doi: 10.1158/0008-5472.CAN-09-2249
Supplementary Material	Access the most recent supplemental material at: http://cancerres.aacrjournals.org/content/suppl/2010/01/26/0008-5472.CAN-09-2249.DC1

Cited articles	This article cites 37 articles, 17 of which you can access for free at: http://cancerres.aacrjournals.org/content/70/3/1236.full#ref-list-1
-----------------------	--

Citing articles	This article has been cited by 6 HighWire-hosted articles. Access the articles at: http://cancerres.aacrjournals.org/content/70/3/1236.full#related-urls
------------------------	---

E-mail alerts	Sign up to receive free email-alerts related to this article or journal.
----------------------	--

Reprints and Subscriptions	To order reprints of this article or to subscribe to the journal, contact the AACR Publications Department at pubs@aacr.org .
-----------------------------------	--

Permissions	To request permission to re-use all or part of this article, use this link http://cancerres.aacrjournals.org/content/70/3/1236 . Click on "Request Permissions" which will take you to the Copyright Clearance Center's (CCC) Rightslink site.
--------------------	--